

# Collective Modes of an Anisotropic Quark-Gluon Plasma

Paul Romatschke and Michael Strickland

Institut für Theoretische Physik, Technische Universität Wien,  
Wiedner Hauptstrasse 8-10, A-1040 Vienna, Austria

## Abstract

We analyze the collective modes of high-temperature QCD in the case when there is an anisotropy in the momentum-space distribution function for the gluons. We perform a tensor decomposition of the gluon self-energy and solve the dispersion relations for both stable and unstable modes. Results are presented for a class of anisotropic distribution functions which can be obtained by stretching or squeezing an isotropic distribution function along one direction in momentum space. We find that there are three stable modes and either one or two unstable modes depending on whether the distribution function is stretched or squeezed. The presence of unstable modes which have exponential growth can lead to a more rapid thermalization and isotropization of the soft modes in a quark-gluon plasma and therefore may play an important role in the dynamical evolution of a quark-gluon plasma.

PACS numbers: 11.15Bt, 04.25Nx, 11.10Wx, 12.38Mh

## I. INTRODUCTION

In the ongoing ultra-relativistic heavy collision experiments at the Relativistic Heavy Ion Collider (RHIC) and the upcoming ones at the Large Hadron Collider (LHC) the behavior of nuclear matter under extreme conditions will be studied. The hope of these experiments is to create temperatures which are high enough for nuclear matter to undergo a phase transition to a quark gluon plasma (QGP). The quark gluon plasma, if generated, is expected to expand, cool, and then hadronize in the final stage of its evolution. In this context, an outstanding question faced by experimentalists and theorists is whether or not the system will "thermalize" fast enough to allow a thermodynamic description of the system during the central part of its evolution.

In this paper we study the role of the collective modes of finite-temperature QCD in the thermalization, particularly the isotropization, of a finite-temperature QGP with anisotropic momentum-space distribution functions. This question has been addressed in previous papers in which the existence of instabilities of a QGP were studied. In Refs. [1, 2, 3] Morozynski discussed the existence of instabilities to chromomagnetic fluctuations with a particular orientation of the chromoelectric field and wave-vector. In those papers Morozynski showed that there existed an instability which was the equivalent of the Weibel or filamentation instability in electrodynamics [4]. Weibel showed in his original paper that, within electrodynamics, unstable transverse modes exist in plasma with anisotropic momentum distributions and he also derived their rate of growth in linear response theory. These types of instabilities are potentially very important to QGP evolution at RHIC or LHC due to the large amount of momentum-space anisotropy in the gluon distribution functions at  $t = 1 \text{ fm}/c$ .

Morozynski and Randrup have recently performed phenomenological estimates of the growth rate of the instabilities for two types of anisotropic distribution functions [5]. They found that the degree of amplification of the Weibel instability is not expected to dominate the dynamics of a QGP instead being comparable to the contribution from elastic Boltzmann collisions. However, they did point out that since a large number of the unstable modes could be excited then it is possible that their combined effect on the overall dynamics could be significant. In this paper we perform a detailed study of the hard-thermal-loop resummed gluon self-energy including a complete tensor decomposition of the self-energy and identification of all stable and unstable collective modes.

In Sec. II we set up the framework used to obtain the hard-thermal-loop self-energy in a system with an anisotropic momentum-space distribution. In Sec. III we present a tensor decomposition of the self-energy and dielectric tensors. In Sec. IV we work out the details of the tensor decomposition and give expressions for the self-energy "structure functions." In Sec. V we discuss the static limit of the various self-energy structure functions. In Sec. VI we use the tensor decomposition of the dielectric tensor to determine dispersion relations for all stable and unstable modes. In Sec. VII we present analytic expressions for the self-energy structure functions in the small-anisotropy limit. Finally, in Sec. VIII we present conclusions and outlook for application of the results found here. We provide a summary of our notational conventions and expressions for the various self-energy structure functions in two appendices.

## II. HARD-THERMAL-LOOP SELF-ENERGY

We begin by repeating some of the steps necessary to derive the hard-thermal-loop resummed gluon self-energy within semi-classical transport theory [1, 2, 3]. Within this approach partons are

described by their phase-space densities and their time evolution is given by Vlasov-type transport equations [6, 7]. In this paper we will concentrate on the physics at the soft scale,  $k \sim gT \ll T$ , which is the first scale at which collective motion appears. At this scale the magnitude of the field fluctuations is  $A \sim \sqrt{gT}$  and derivatives are of the scale  $\partial_x \sim gT$ . With this power-counting a systematic truncation of the terms contributing to the transport equations for soft momenta can be realized.

At leading order in the coupling constant the color current,  $J$ , induced by a soft gauge field,  $A$ , with four-momentum  $K = (!; k)$  can be obtained by performing a covariant gradient expansion of the quark and gluon Wigner functions in mean-field approximation. The result is

$$J_{\text{ind}}^a(X) = g \int \frac{d^3p}{(2\pi)^3} V_{(2\pi)^3} (2N_c N^a(p;X) + N_f (n_+^a(p;X) - n_-^a(p;X))) ; \quad (1)$$

where  $V_{(2\pi)^3} = (1; k=!)$  is the gauge field four-velocity,  $N^a(p;X)$  is the fluctuating part of the gluon density, and  $n_+^a(p;X)$  and  $n_-^a(p;X)$  are the fluctuating parts of the quark and anti-quark densities, respectively. Note that  $N^a$  transforms as a vector in the adjoint representation ( $N \rightarrow N^a T^a$ ) and  $n^a$  transforms as a vector in the fundamental representation ( $n \rightarrow n^a t^a$ ).

The quark and gluon density matrices above satisfy the following transport equations

$$[D_X; n(p;X)] = -gV F_{(p;X)} \otimes n(p); \quad (2)$$

$$[D_X; N(p;X)] = -gV F_{(p;X)} \otimes N(p); \quad (3)$$

where  $D_X = \partial_X + igA(X)$  is the covariant derivative.

Solving the transport equations (2) and (3) for the fluctuations  $N$  and  $n$  gives the induced current via Eq. (1)

$$J_{\text{ind}}(X) = g^2 \int \frac{d^3p}{(2\pi)^3} V_{(2\pi)^3} \partial_{(p)} f(p) \cdot \int U(X;X-V) F(X-V) U(X-V;X); \quad (4)$$

where  $U(X;Y)$  is a gauge parallel transporter defined by the path-ordered integral

$$U(X;Y) = P \exp \left( -ig \int_X^Y dZ A(Z) \right); \quad (5)$$

$F_{(p)} = \partial A - \partial A - ig[A;A]$  is the gluon field strength tensor, and

$$f(p) = 2N_c N(p) + N_f (n_+(p) + n_-(p)); \quad (6)$$

Neglecting terms of subleading order in  $g$  (implying  $U \approx 1$  and  $F \approx \partial A - \partial A$ ) and performing a Fourier transform of the induced current to momentum space we obtain

$$J_{\text{ind}}(K) = g^2 \int \frac{d^3p}{(2\pi)^3} V_{(2\pi)^3} \partial_{(p)} f(p) \cdot g \frac{V \cdot K}{K \cdot V + i\epsilon} A(K); \quad (7)$$

where  $\epsilon$  is a small parameter that has to be sent to zero in the end.

From this expression of the induced current the self-energy is obtained via

$$\Pi(K) = \frac{J_{\text{ind}}(K)}{A(K)}; \quad (8)$$

which gives

$$\Pi(K) = g^2 \int \frac{d^3p}{(2\pi)^3} V_{(2\pi)^3} \partial_{(p)} f(p) \cdot g \frac{V \cdot K}{K \cdot V + i\epsilon}; \quad (9)$$

This tensor is symmetric,  $\Pi^{ij}(K) = \Pi^{ji}(K)$ , and transverse,  $K_i \Pi^{ij}(K) = 0$ . Note that the same result can be obtained using diagrammatic methods if one assumes that the distribution function is symmetric under  $\mathbf{p} \rightarrow -\mathbf{p}$  [8].

In the linear approximation the equation of motion for the gauge fields can be obtained by expressing the induced current in terms of the self-energy

$$J_{\text{ind}}^i(K) = \Pi^{ij}(K) A_j(K); \quad (10)$$

and plugging this into Maxwell's equation

$$iK_\mu F^{\mu\nu}(K) = J_{\text{ind}}^\nu(K) + J_{\text{ext}}^\nu(K); \quad (11)$$

to obtain

$$[K^2 g^{\mu\nu} - K^\mu K^\nu + \Pi^{\mu\nu}(K)] A_\nu(K) = J_{\text{ext}}^\mu(K); \quad (12)$$

where  $J_{\text{ext}}$  is an external current. Using the gauge invariance of the self-energy we can write this in terms of a physical electric field by specifying a particular gauge. In the temporal axial gauge defined by  $A_0 = 0$  we obtain

$$[(k^2 - \Pi^{ij}(k)) E^j(K)] = i J_{\text{ext}}^i(K); \quad (13)$$

Inverting the propagator allows us to determine the response of the system to the external source

$$E^i(K) = i [K^2 - \Pi^{ij}(K)]^{-1} J_{\text{ext}}^j(K); \quad (14)$$

The dispersion relations for the collective modes can be obtained by finding the poles in the propagator  $\Pi^{ij}(K)$ .

### III. TENSOR DECOMPOSITION

In this section we develop a tensor basis for an anisotropic system in which there is only one preferred direction. As mentioned above the self-energy is symmetric and transverse. As a result not all components of  $\Pi^{ij}$  are independent and we can restrict our considerations to the spatial part of  $\Pi^{ij}$ , denoted  $\Pi^{ij}$ . We therefore need to construct a basis for a symmetric 3-tensor that { apart from the momentum  $k^i$  { also depends on a fixed anisotropy three-vector  $n^i$ , with  $n^2 = 1$ . Following Ref. [9] we first define the projection operator

$$A^{ij} = \Pi^{ij} - k^i k^j / k^2; \quad (15)$$

and use it to construct  $\Pi^{ij} = A^{ij} n^j$  which obeys  $\Pi^{ij} k_j = 0$ . With this we can construct the remaining three tensors

$$B^{ij} = k^i k^j / k^2 \quad (16)$$

$$C^{ij} = n^i n^j / n^2 \quad (17)$$

$$D^{ij} = k^i n^j + k^j n^i; \quad (18)$$

Any symmetric 3-tensor  $T$  can now be decomposed into the basis spanned by the four tensors  $A$ ;  $B$ ;  $C$ ; and  $D$

$$T = aA + bB + cC + dD; \quad (19)$$

Furthermore, the inverse of any such tensor is then given as

$$T^{-1} = a^{-1}A + \frac{(a+c)B - a^{-1}(bc - n^2 k^2 d^2)C - dD}{b(a+c) - n^2 k^2 d^2}; \quad (20)$$

#### IV. SELF-ENERGY STRUCTURE FUNCTIONS

The spacelike components of the self-energy tensor can be written as

$$\Pi^{ij}(K) = \frac{g^2}{(2\pi)^3} \int d^3p v^i v^j f(p) + \frac{v^j k^1}{K(V+i)} ; \quad (21)$$

At this point the distribution function  $f(p)$  is completely arbitrary. In order to proceed we need to specify a form for the distribution function. In what follows we will assume that  $f(p)$  can be obtained from an arbitrary isotropic distribution function by the rescaling of only one direction in momentum space. In practice this means that, given any isotropic distribution function  $f_{\text{iso}}(p^2)$ , we can construct an anisotropic version by changing the argument

$$f(p) = f_{\text{iso}}(p^2 + (p \cdot \hat{n})^2) ; \quad (22)$$

where  $\hat{n}$  is the direction of the anisotropy and  $\alpha > 1$  is a adjustable anisotropy parameter. Note that  $\alpha > 0$  corresponds to a contraction of the distribution in the  $\hat{n}$  direction whereas  $-1 < \alpha < 0$  corresponds to a stretching of the distribution in the  $\hat{n}$  direction. This assumption allows us to simplify (21) by performing a change of variables to  $\tilde{p}$

$$\tilde{p}^2 = p^2 + (p \cdot \hat{n})^2 ; \quad (23)$$

After making this change of variables it is possible to integrate out the  $\tilde{p}_j$  dependence giving

$$\Pi^{ij}(K) = m_D^2 \int \frac{d^3p}{4} v^i v^j \frac{v^1 + (v \cdot \hat{n})n^1}{(1 + (v \cdot \hat{n})^2)^2} + \frac{v^j k^1}{K(V+i)} ; \quad (24)$$

where

$$m_D^2 = \frac{g^2}{2\pi^2} \int_0^1 dp p^2 \frac{df_{\text{iso}}(p^2)}{dp} ; \quad (25)$$

We can then decompose the self-energy into four structure functions

$$\Pi^{ij} = A^{ij} + B^{ij} + C^{ij} + D^{ij} ; \quad (26)$$

which are determined by taking the following contractions:

$$\begin{aligned} k^i \Pi^{ij} k^j &= k^2 A ; \\ \hat{n}^i \Pi^{ij} k^j &= \hat{n}^2 k^2 B ; \\ \hat{n}^i \Pi^{ij} \hat{n}^j &= \hat{n}^2 (C + D) ; \\ \text{Tr} \Pi^{ij} &= 2A + C + D ; \end{aligned} \quad (27)$$

In Appendix B we collect the resulting integral expressions for the structure functions. All four structure functions depend on  $m_D$ ,  $\alpha$ ,  $k$ ,  $\hat{n}$ , and  $\hat{k} \cdot \hat{n} = \cos \theta$ . In the limit  $\alpha \rightarrow 0$  the structure functions  $A$  and  $B$  reduce to the isotropic hard-thermal-loop self-energies and  $C$  and  $D$  vanish

$$\begin{aligned} A(K;0) &= A_T(K) ; \\ B(K;0) &= \frac{\alpha^2}{k^2} A_L(K) ; \\ C(K;0) &= 0 ; \\ D(K;0) &= 0 ; \end{aligned} \quad (28)$$

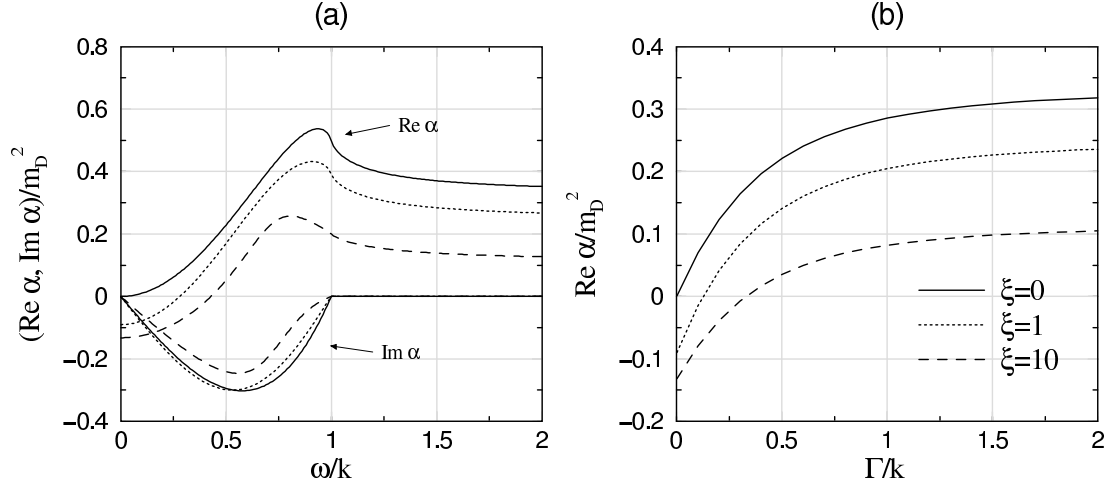


FIG. 1: Real and imaginary parts of  $\alpha = m_D^2$  as a function of real  $\omega/k$  are shown in (a) and in (b) the real part of  $\alpha = m_D^2$  is shown for  $\omega/k = i\Gamma/k$  with  $\xi = 0, 1, 10$  in both cases.

with

$$\tau(K) = \frac{m_D^2}{2} \frac{k^2}{k^2} \left[ 1 - \frac{k^2}{2k} \log \frac{k + k}{k} \right]; \quad (29)$$

$$L(K) = m_D^2 \frac{k}{2k} \log \frac{k + k}{k} \left[ 1 - \frac{k^2}{2k} \log \frac{k + k}{k} \right]; \quad (30)$$

For finite  $\xi$  the analytic structure of the structure functions is the same as in the isotropic case. There is a cut in the complex  $k$  plane which we can choose to run along the real  $k$  axis from  $k < k < k$ . For real-valued  $k$  the structure functions are complex for all  $k < k$  and real for  $k > k$ . For imaginary-valued  $k$  all four structure functions are real-valued. In Fig. 1 we plot the structure function for real and imaginary values of  $k$ ,  $\xi = 0, 1, 10$ , and  $\xi = 4$ .

With these structure functions in hand we can construct the propagator  $\chi_{ij}(K)$  using the expressions from the previous section. Writing  $\chi^i(K)$  in terms of our tensor basis

$$\chi^i(K) = (k^2 - k^2 + \xi)A + (\xi k^2)B + C + D \quad (31)$$

and applying the inversion formula (20) we obtain an expression for the propagator

$$\chi(K) = A_A + (k^2 - k^2 + \xi) G_B + [(k^2 - k^2) G_A C + G_D]; \quad (32)$$

with

$$A_A^1(K) = k^2 - k^2 + \xi; \quad (33)$$

$$G_A^1(K) = (k^2 - k^2 + \xi)(k^2 - k^2) k^2 n^2; \quad (34)$$

Note that we can reorganize  $\chi(K)$  and write it as

$$\chi(K) = A [A - C] + G [(k^2 - k^2 + \xi)B + (\xi k^2)C - D]; \quad (35)$$

## V. STATIC LIMIT

In order to see how the momentum-space anisotropy in the distribution functions affects the response to static electric and magnetic fluctuations we examine the limit  $k \rightarrow 0$  of the propagators

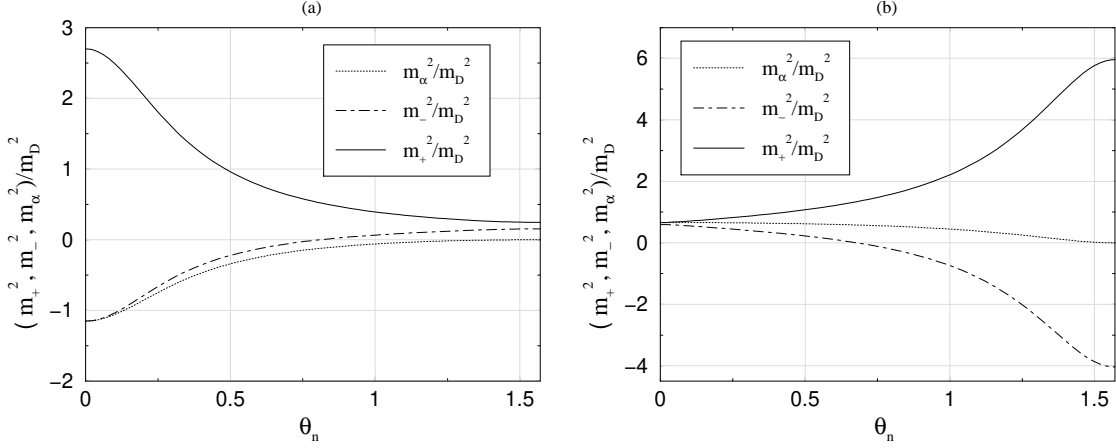


FIG. 2: Angular dependence of  $m_+^2$ ,  $m_-^2$ , and  $m_\alpha^2$  at fixed (a)  $\alpha = 10$  and (b)  $\alpha = 0.9$ .

(33) and (34). Approaching along the real  $k$  axis we find that to leading order  $\mathcal{O}(k^0)$ ,  $\mathcal{O}(k^2)$ , and  $\mathcal{O}(ik)^1$ : We can therefore define four mass scales

$$\begin{aligned}
 m^2 &= \lim_{k \rightarrow 0} \quad ; \\
 m^2 &= \lim_{k \rightarrow 0} \frac{k^2}{k^2} \quad ; \\
 m^2 &= \lim_{k \rightarrow 0} \quad ; \\
 m^2 &= \lim_{k \rightarrow 0} \frac{\text{Re } k^2}{k^2} \text{Im} \quad :
 \end{aligned} \tag{36}$$

Writing the static limit of the propagators (33) and (34) in terms of these masses gives

$$A^{-1} = k^2 + m^2 \tag{37}$$

$$G^{-1} = \frac{1}{k^2} (k^2 + m^2 + m^2) (k^2 + m^2) - m^4 \quad : \tag{38}$$

$G^{-1}$  can be factorized into

$$G^{-1} = \frac{1}{k^2} (k^2 + m_+^2) (k^2 + m_-^2) \quad ; \tag{39}$$

where

$$2m^2 = M^2 - \frac{q}{M^4 - 4(m^2(m^2 + m^2) - m^4)} \quad ; \tag{40}$$

with

$$M^2 = m^2 + m^2 + m^2 \quad : \tag{41}$$

In the isotropic limit,  $k \rightarrow 0$ ,  $m^2 = m^2 = m^2 = m^2 = 0$  and  $m_+^2 = m_D^2$ . For finite  $k$  it is possible to evaluate all four masses defined above analytically. The results for  $m$  and  $m$  are listed in Appendix B. In Fig. 2 we plot the angular dependence of  $m^2$ ,  $m_+^2$ , and  $m^2$  at fixed  $\alpha = 10$  and  $\alpha = 0.9$ . In the case  $\alpha > 0$  (Fig. 2a) we see that for small  $k_n$  the scale  $m_+^2 \rightarrow m_D^2$  and for  $k_n$  near  $\pi/2$ ,  $m_+^2 \rightarrow m_D^2$ . For small  $k_n$  the scales  $m^2$  and  $m^2$  are negative. The fact that  $m$  and  $m$  are non-vanishing is in agreement with the findings of Cooper et al. [10]; however, they neglected

<sup>1</sup> Identical results can be obtained by coming in along the imaginary axis with a suitable redefinition of  $m^2$ .

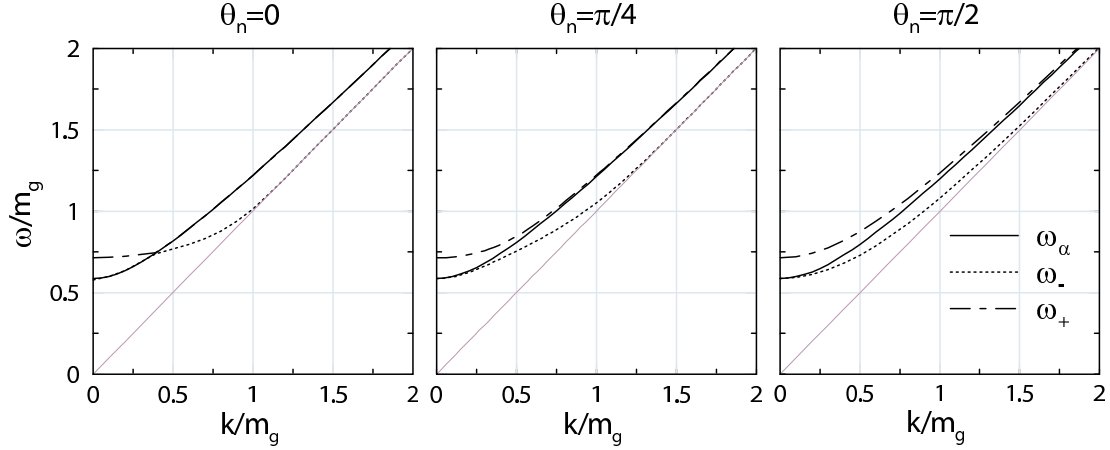


FIG. 3: Angular dependence of  $\omega_-$ ,  $\omega_+$ , and  $\omega_\alpha$  for  $m_g = m_D = \frac{p_-}{3}$ ,  $\mu = 10$ , and  $\theta_n = 0; \pi/4; \pi/2$ .

to consider the fact that these masses might be negative and would therefore not correspond to screening of the magnetic interaction. The fact that these quantities are negative indicates that for  $\mu > 0$  the system possesses an instability to transverse and "mixed" external perturbations associated with  $m_-^2$  and  $m_+^2$ , respectively. The transverse instability is present for any  $\theta_n \neq \pi/2$  while the mixed instability is only present for  $\theta_n < \theta_n^{\text{mixed}}$  with  $\theta_n^{\text{mixed}}$  depending on the value of  $\mu$ . In the case  $\mu < 0$  (Fig. 2b) we see that for small  $\theta_n$  the scale  $m_+^2 \approx m_D^2$  and for  $\theta_n$  near  $\pi/2$ ,  $m_+^2 \approx m_D^2$ . For  $\theta_n > \pi/4$  the scale  $m_-^2$  is negative again signaling the presence of an instability in the system. In the next section we will discuss these instabilities in more detail.

## VI. COLLECTIVE MODES

A similar factorization of  $\chi_G^{-1}$  can be achieved in the non-static case allowing us to determine the dispersion relations for all of the collective modes in the system.

### A. Stable Modes

First, let's consider the stable collective modes which have poles at real-valued  $\omega > k$ . In this case we factorize  $\chi_G^{-1}$  as

$$\chi_G^{-1} = (\omega^2 - \omega_+^2)(\omega^2 - \omega_-^2); \quad (42)$$

where

$$\omega_{\pm}^2 = \frac{\mu}{4} \frac{4((\mu + k^2) \pm k^2 n^2)}{4((\mu + k^2) \pm k^2 n^2)}; \quad (43)$$

and

$$\omega^2 = \mu + k^2; \quad (44)$$

Note that the quantity under the square root in (43) can be written as  $((\mu + k^2) \pm k^2 n^2)^2 + 4k^2 n^2$  which is always positive for real  $\omega > k$ . Therefore there are at most two stable modes coming from  $\chi_G$ .

The remaining stable collective mode comes from the zero of  $\chi_A^{-1}$ . The dispersion relations for all of the collective modes can be determined by finding the solutions to

$$\omega^2 = \mu (\omega^2 - k^2); \quad (45)$$



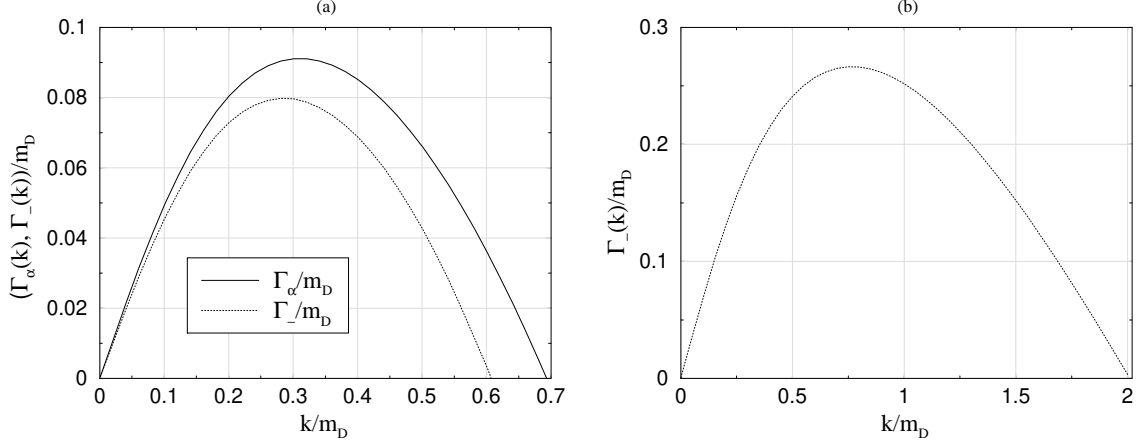


FIG. 4:  $\Gamma_\alpha(k)$  and  $\Gamma_-(k)$  as a function of  $k$  with (a)  $\omega = 10$  and  $n = -8$  and (b)  $\omega = 0.9$  and  $n = -2$ .

$$\omega^2 = k^2 + (\omega^2) : \quad (46)$$

In the isotropic limit (28)  $\omega = \omega_+ = \omega_T$  and  $\omega = \omega_-$ . For finite  $n$  there are three stable quasiparticle modes with dispersion relations which depend on the angle of propagation with respect to the anisotropy vector,  $\hat{n}$ . In Fig. 3 we plot the dispersion relations for all three modes for  $m_D = \frac{1}{3}$ ,  $\omega = 10$ , and  $n = 0; -4; -2$ .

### B. Unstable Modes

For non-zero  $n$  the propagator also has poles along the imaginary  $\omega$  axis.<sup>2</sup> The dispersion relation for these modes can be determined by taking  $\omega = i$  with  $k$  real-valued and solving for  $k$ . In this case we factorize the inverse propagator as

$$G^{-1} = (\omega^2 + \omega_+^2)(\omega^2 + \omega_-^2); \quad (47)$$

where  $\omega_\pm$  on the right hand side are evaluated at  $\omega = i$ . However, in contrast to the stable modes there is at most one solution in this case since numerically we find that  $\omega_+^2 > 0$  for all  $n > 0$ .

For  $n > 0$  there is also an unstable mode present in  $\omega_A$  so that in this case there are two unstable modes in the system which can be found by solving

$$\omega^2 = \omega_+^2(i); \quad (48)$$

$$\omega^2 = k^2(i); \quad (49)$$

Note that in both cases there are two solutions corresponding to modes with positive and negative growth rates. One of these corresponds to an exponentially growing solution and the other an exponentially decaying one. In Fig. 4a we plot  $\Gamma_\alpha(k)$  and  $\Gamma_-(k)$  with  $\omega = 10$  and  $n = -8$ . For

$\omega < 0$  there is no longer an unstable mode coming from  $\omega_A$  and there is therefore only one unstable mode coming from  $\omega_-$ . In Fig. 4b we plot  $\Gamma_-(k)$  with  $\omega = 0.9$  and  $n = -2$ .

<sup>2</sup> We have checked for poles at complex  $\omega$  numerically but found none.

## V II. S M A L L E X P A N S I O N

In the small- limit it is possible to obtain analytic expressions for all of the structure functions order-by-order in . To linear order in

$$\begin{aligned}
 &= T(z) + \frac{z^2}{12} (3 + 5 \cos 2\theta_n) m_D^2 - \frac{1}{6} (1 + \cos 2\theta_n) m_D^2 \\
 &\quad + \frac{1}{4} T(z) (1 + 3 \cos 2\theta_n) z^2 (3 + 5 \cos 2\theta_n) ; \\
 z^2 &= L(z) + \frac{1}{6} (1 + 3 \cos 2\theta_n) m_D^2 + L(z) \cos 2\theta_n - \frac{z^2}{2} (1 + 3 \cos 2\theta_n) ; \\
 &= \frac{1}{3} (3 T(z) - m_D^2) (z^2 - 1) \sin^2 \theta_n ; \\
 &= \frac{1}{3k} (4z^2 m_D^2 + 3 T(z) (1 - 4z^2)) \cos \theta_n ; \tag{50}
 \end{aligned}$$

where  $z = \frac{1}{k}$ .

### A . S t a t i c L i m i t

Using the linear expansions and the fact that in the static limit  $L \rightarrow m_D^2$  and  $T \rightarrow 1$  if  $k \rightarrow 0$  we can write for the masses (36)

$$\begin{aligned}
 m^2 &= \frac{1}{6} (1 + \cos 2\theta_n) ; \\
 m^2 &= 1 + \frac{1}{6} (3 \cos 2\theta_n - 1) ; \\
 m^2 &= \frac{1}{3} \sin^2 \theta_n ; \\
 m^2 &= \frac{1}{4} \sin \theta_n \cos \theta_n ; \tag{51}
 \end{aligned}$$

where  $m^2 = m^2 = m_D^2$ . Using these we can obtain small- expressions for  $m$  defined in (40)

$$\begin{aligned}
 m_+^2 &= 1 + \frac{1}{6} (3 \cos 2\theta_n - 1) ; \\
 m^2 &= \frac{1}{3} \cos 2\theta_n : \tag{52}
 \end{aligned}$$

### B . C o l l e c t i v e M o d e s

Since  $\epsilon \rightarrow 0$  it can be ignored in the expansion of (43) so that to linear order in the collective modes satisfy

$$\begin{aligned}
 A^1 &= k^2 \epsilon^2 + \epsilon = 0 \\
 G^1 &= (k^2 \epsilon^2 + \epsilon + \epsilon) (\epsilon^2) = 0 ; \tag{53}
 \end{aligned}$$

where  $\epsilon$ ,  $\epsilon$ , and  $\epsilon$  are given by (50). Note again that there is only one unstable mode coming from  $G^1$  since  $\epsilon > 0$  for all  $k > 0$ .

### V III. C O N C L U S I O N S

In this paper we have derived a tensor basis for the gluon self-energy in a high-temperature quark gluon plasma with an anisotropic momentum-space distribution. We then restricted the distribution function by requiring that it could be obtained from an isotropic distribution function by the rescaling of one direction specified by an anisotropy vector,  $\hat{n}$ , and strength,  $\beta$ . Positive values of  $\beta$  correspond to a contraction of the isotropic distribution function along  $\hat{n}$  while negative values of  $\beta$  correspond to a stretching along  $\hat{n}$ . Within this framework we could derive analytic forms for all of the structure functions associated with the tensor basis. Using these expressions we were then able to identify and determine the dispersion relations for the collective modes for both positive and negative  $\beta$ . We found that for  $\beta > 0$  there were at most three stable and two unstable modes with dispersion relations which depended on the angle between the wave vector,  $k$ , and the anisotropy vector. For  $\beta < 0$  we found that there were also three stable modes but only one unstable mode. Additionally, we obtained analytic expressions for the structure functions in the limit of small  $\beta$ . These results should provide a reference point for the systematic study of the isotropization of a relativistic plasma.

The study of Morozynski and Randrup suggests that during heavy-ion collisions the rate of isotropization via collective modes is comparable with collisions and therefore cannot be ignored [5]. In this paper we have made no attempt to discuss the phenomenological rate for instability growth because there are a number of questions which would need to be addressed prior to making any definitive statements about the role of instabilities in plasma evolution and their expected contribution to observables. This is because we have only derived the self-energy in a linear expansion in the fluctuations and to leading-order in the coupling constant. Assuming that there is truly exponential growth of the fields in the direction of the anisotropy this means that the linear approximation will break down very quickly. In practice the non-linear terms in the transport equations will become important and regulate the growth of the modes which have become unstable.

Within electrodynamics the coupling constant is small and it is possible to experimentally study the Weibel instability [11]. However, with QCD the story is dramatically different since for experimentally realizable situations the coupling constant is large and the non-linear effects due to gluon self-interaction become important much sooner than any non-linear effects would for QED. Nevertheless, this does not diminish from the fact that these unstable modes exist and will therefore have a role to play in plasma evolution. In order to assess this role, however, detailed studies of the time evolution of anisotropic quark-gluon plasmas will need to be performed.

#### A cknow ledgm ents

M.S. and P.R. would like to thank S. Morozynski and A. Rebhan for discussions. M.S. was supported by an Austrian Science Fund (FWF) Lise Meitner fellowship M 689. P.R. was supported by the Austrian Science Fund Project No. P 14632.

### A P P E N D I X A : N O T A T I O N A N D C O N V E N T I O N S

We summarize here the notation and conventions which we use in the main body of the text.

Natural units:  $\hbar = c = 1$

Metric:  $g = g_{\mu\nu} = \text{diag}(1; -1; -1; -1)$

4-vectors: Indicated by Greek indices, e.g.  $K = (\omega; \mathbf{k})$ .

3-vectors: Indicated by lowercase Latin characters. Upper Latin indices like  $i, j, k$  use a Euclidean 3-metric, e.g.  $\mathbf{k} = k^i, k^i k^i = k^2$ .

Fourier transform :

$$j(\mathbf{K}) = \int d^4X e^{i\mathbf{K} \cdot \mathbf{X}} j(\mathbf{X})$$

$$j(\mathbf{X}) = \int \frac{d^4K}{(2\pi)^4} e^{-i\mathbf{K} \cdot \mathbf{X}} j(\mathbf{K})$$

## APPENDIX B: ANALYTIC EXPRESSIONS FOR STRUCTURE FUNCTIONS

In this appendix we collect the integral and analytic expressions for the structure functions  $\chi_1$ ,  $\chi_2$ ,  $\chi_3$ , and  $\chi_4$ . Choosing  $n = \hat{z}$  and  $\mathbf{k}$  to lie in the  $x-z$  plane ( $k_x = k_z = \tan \theta_n$ ) we have  $v_n = \cos \theta_n$  and  $\mathbf{v} \cdot \mathbf{k} = k_x \cos \theta_n \sin \theta_n + k_z \cos \theta_n$ . Using this parameterization the integration in all four structure functions defined by the contractions in Eq. (27) can be performed analytically.

$$\chi_1(\mathbf{K}; \mathbf{v}) = \frac{m_D^2}{k^2 n^2} \int \frac{d(\cos \theta)}{2} \frac{1 + \frac{k_z \cos \theta}{k^2}}{(1 + (\cos \theta)^2)^2} \left[ k_z \cos \theta + k^2 (s^2 - (\cos \theta \frac{k_z}{k^2})^2) R(\frac{k_z \cos \theta}{k^2}; k_x \sin \theta) \right]; \quad (\text{B.1})$$

$$\chi_2(\mathbf{K}; \mathbf{v}) = \frac{m_D^2}{k^2} \int \frac{d(\cos \theta)}{2} \frac{1}{(1 + (\cos \theta)^2)^2} \left[ 1 - (\frac{k_z \cos \theta}{k^2}) R(\frac{k_z \cos \theta}{k^2}; k_x \sin \theta) \right]; \quad (\text{B.2})$$

$$\chi_3(\mathbf{K}; \mathbf{v}) = m_D^2 \int \frac{d(\cos \theta)}{2} \frac{1}{k^2 (1 + \cos^2 \theta)^2} \left[ 1^2 + k^2 \cos^2 \theta - \frac{k^2}{k_x^2} (1^2 - k_z^2 \cos^2 \theta) + \frac{(\frac{k_z \cos \theta}{k^2})^4}{k_x^2} - 2 (\cos \theta \frac{k_z}{k^2})^2 s^2 R(\frac{k_z \cos \theta}{k^2}; k_x \sin \theta) \right]; \quad (\text{B.3})$$

$$\chi_4(\mathbf{K}; \mathbf{v}) = \frac{m_D^2}{k^4 n^2} \int \frac{d(\cos \theta)}{2} \frac{1 + \frac{k_z \cos \theta}{k^2}}{(1 + \cos^2 \theta)^2} k_z + (k^2 \cos^2 \theta - k_z^2) R(\frac{k_z \cos \theta}{k^2}; k_x \sin \theta); \quad (\text{B.4})$$

where  $s^2 = (1 - \cos^2 \theta) (k_x^2 = k^2)$  and

$$R(a; b) = \int_0^{\frac{\pi}{2}} \frac{d\theta}{2} \frac{1}{a - b \cos \theta + i} = \frac{1}{a + b + i} \frac{1}{a - b + i}; \quad (\text{B.5})$$

When  $a$  and  $b$  are real-valued  $R$  can be simplified to

$$R(a; b) = \frac{\text{sgn}(a) (a^2 - b^2)}{a^2 - b^2} \frac{i (b^2 - a^2)}{b^2 - a^2}; \quad (\text{B.6})$$

with  $\theta(x)$  being the usual step-function. Note that the remaining integration over  $\theta$  can also be done analytically but the results are rather unwieldy so we do not list them here.

# STATIC LIMIT

In the limit  $\omega \rightarrow 0$  it is possible to obtain analytic expressions for all four structure functions. The results for  $m^2$  and  $m^2$  defined in Eq. (36) are

$$m^2 = \frac{m_D^2}{2k_x^2} \left[ k_z^2 \arctan \frac{p_-}{k^2 + k_x^2} - \frac{k_z k^2}{k^2 + k_x^2} \arctan \frac{p_- k_z}{k^2 + k_x^2} \right]; \quad (B.7)$$

$$m^2 = m_D^2 \frac{\left( \frac{p_-}{k^2 + k_x^2} + (1 + \frac{k^2}{k_x^2}) \arctan \frac{p_-}{k^2 + k_x^2} \right) (k^2 + k_x^2) + k_z k_z \frac{p_-}{k^2 + k_x^2} + \frac{k^2 (1 + \frac{k^2}{k_x^2})}{k^2 + k_x^2} \arctan \frac{p_- k_z}{k^2 + k_x^2}}{2 \frac{p_-}{k^2 + k_x^2} (1 + \frac{k^2}{k_x^2}) (k^2 + k_x^2)}; \quad (B.8)$$

with similar results for  $m^2$  and  $m^2$ .

- 
- [1] S.M rowczynski, Phys.Lett.B 314, 118 (1993).
  - [2] S.M rowczynski, Phys.Rev.C 49, 2191 (1994).
  - [3] S.M rowczynski, Phys.Lett.B 393, 26 (1997).
  - [4] E.S.W eibel, Phys.Rev.Lett. 2, 83 (1959).
  - [5] J.Randrup and S.M rowczynski, arXiv: nucl-th/0303021, (2003).
  - [6] H.T.Elze and U.Heinz, Phys.Rep. 183, 81 (1989).
  - [7] J.P.Blaizot and E.Iancu, Phys.Rep. 359, 355 (2002)
  - [8] S.M rowczynski and M.H.Thoma, Phys.Rev.D 57, 036011 (2000).
  - [9] R.Kobes, G.Kunstatter, and A.Rebhan, Nucl.Phys.B 355, 1 (1991).
  - [10] F.Cooper, C.-W.Kao, and G.C.Nayak, arXiv: hep-ph/0207370, (2002).
  - [11] M.S.Wei, et al., "Experimental Observations of the Weibel Instability in High Intensity Laser Solid Interactions", Central Laser Facility (UK) Annual Report, (2002).